Available online at www.sciencedirect.com
SCIENCE DIRECT®
Journal of Nuclear Materials 323 (2003) 213–219
journal of nuclear materials
www.elsevier.com/locate/jnucmat

SIA activity during irradiation of nanocrystalline Ni

M. Samaras [a], P.M. Derlet [a], H. Van Swygenhoven [a,*], M. Victoria [b]

[a] Paul Scherrer Institute, CH-5232 Villigen, Switzerland
[b] CRPP-Fusion Technology Materials, EPFL, CH-5232 Villigen-PSI, Switzerland

Abstract

Cascade damage simulations in a 12 nm nanocrystalline Ni sample are presented. Sinks present in the sample such as grain boundaries and vacancy defects influence the movement of self-interstitial atoms (SIAs). Two temporal mechanisms of SIA activity during their movement to GBs are distinguished: replacement collision sequences and 1D/3D thermal motion. Clustering of SIAs is biased by nearby GBs, forming SIA clusters at the large limit of that seen in displacement cascades of single crystal samples for the same primary knock-on atom energy. SIA clusters containing up to six SIAs are shown to undergo 1D/3D motion due to the presence of the attractive GB sinks in contrast to the traditional picture of purely 1D motion observed for clusters of four or more SIAs in single crystal simulations.

PACS: 61.80.Hg; 81.07.Bc; 02.70.Ns

1. Introduction

Self-interstitial atom (SIA) activity and structure has lead to the belief that SIAs play a dominant role in the final damage state of an irradiated sample [1–3]. The development of a displacement cascade begins with a high kinetic energy primary knock on atom (PKA) imparting its energy ballistically to the surrounding lattice, causing an initially molten and highly disordered region that subsequently cools via dissipative mechanisms such as focusons and replacement collision sequences (RCSs). Focusons dissipate energy without mass transport whereas RCSs lead to the dissipation of energy and mass transport, moving SIAs away from the cascade core region, by a knock-on effect, and transporting SIAs to a point where they are no longer within range to recombine with existing vacancies. The resulting damage state is only a small fraction of the defects produced during the thermal spike phase of cascade development that on cooling return to lattice sites primarily via a non-diffusional recombination process, leaving a vacancy rich core surrounded by SIAs situated at and beyond the periphery of the cascade – thus SIAs and vacancies become spatially segregated.

MD simulations performed on single crystal structures show that SIAs often tend to cluster [1–3]; this compares well with experimental evidence of SIA clustering from X-ray scattering [4]. In single crystal metals, SIAs and SIA clusters have been seen to possess a low activation energy [5,6] that leads to high glissile mobility [7–9] during irradiation; in some cases the larger SIA clusters being more mobile than the point defects [5,10]. Mobility is enhanced by the ease with which SIAs take on a crowdion configuration allowing them to migrate easily [11]. The precise mechanism of the motion of SIAs and SIA clusters during irradiation is still under debate. 1D/3D diffusion is the most recognised theory whereby SIA clusters move along close-packed crystallographic directions [12–14] until thermal activation [15,16] or interactions with other SIA clusters [10] lead to a reorientation of each crowdion to another $\langle 1\,1\,0\rangle$ path. Other theories have been proposed where SIA motion occurs via the propagation of intrinsic kinks [17] or via dissipative 1D Brownian motion [18]. Regardless of the mechanism, the motion of SIA clusters is an efficient mechanism to remove SIAs from the cascade core region [7,8].

* Corresponding author. Tel.: +41-56 310 2931; fax: +41-56 310 3131.
E-mail address: helena.vs@psi.ch (H. Van Swygenhoven).

0022-3115/$ - see front matter © 2003 Elsevier B.V. All rights reserved.
doi:10.1016/j.jnucmat.2003.08.020

Simulations have also shown that pre-existing defects such as dislocations, grain boundaries (GBs), surfaces or vacancy clusters can act as sinks for SIAs. Experiments revealed the special case of GBs acting as a sink for both SIAs and vacancies, resulting in a denuded zone in the vicinity of an interface region [19]. Simulations of single dislocations find that displacement cascade SIAs move via 1D thermal glide to decorate dislocations [20,21] and within a certain 'stand-off distance' are absorbed by the dislocation [21,22] which may be instigated by the rotation of the SIA's Burgers vector or by unfaulting [22]. In comparison, experiment in fcc metals, has shown the presence of only SFT defects within 20 nm of dislocation cores [23,24]. The 'stand-off distance' of clusters containing crowdions has been found to linearly increase with the number of crowdions in the cluster [20,24]. The interaction of an SIA cluster with a dislocation has shown a dependence also on the axis of the SIA cluster compared with the Burgers vector of the dislocation, with the strongest interaction (of edge dislocations in Ni and Fe) occurring when the axis of the crowdion/dumbbell is parallel to the Burgers vector of the dislocation [25]. The influence of general GBs on the production of radiation damage has recently been demonstrated in MD simulations [26–28]. An analogy between the influence of a dislocation and a GB is of interest although limited in its applicability, due to the complex stress and strain fields surrounding GBs (which needs three non-coplanar Burgers vectors of discrete dislocations to obtain the GB Burgers vector content [29]).

The experimental evidence for a denuded zone around a GB, naturally leads to the idea that nanocrystalline (nc) materials, with their high density of GBs and with grain sizes comparable to typical cascade volumes could eventually exhibit an increased radiation resistance. First experiments of ion irradiation in nc-Au [30] and nc-Pd [31] confirmed this idea. Recent atomistic simulation work in nc-Ni employing molecular dynamics (MD) has revealed that the GB does indeed attract SIAs early in the cascade evolution via a replacement collision sequence (RCS) mechanism [26], avoiding the vacancy/interstitial recombination mechanism, and thus leaving behind a vacancy rich defect structure. Hence the primary damage state in an nc material is different from that found in cascade simulations of single crystals. It is expected that vacancies and small vacancy clusters will also eventually arrive at the GB via diffusion. On the other hand, MD simulations in 12 nm grain sized nc Ni have shown that often the dominating vacancy concentration in the nc structure lead to the formation of stacking fault tetrahedra (SFT) already at low cascade energies [32].

The computer generated nc samples used in the present work contain a fully 3D GB network. The most general atomistic definition of what constitutes the GB region are those atoms which do not display the local crystalline symmetry of the associated grains. Using this definition, in computer generated nc samples about 29.2% of atoms belong to the GB for a 5 nm grain size sample, and 15.4% for a 12 nm grain size sample. From an energy analysis, it is found that with decreasing grain size, there is a negligible grain size dependence on the local GB cohesive energy down to grain diameters of 3 nm [33], and via a pair-distribution-function analysis of the GB atoms no significant disorder is apparent akin to an amorphous phase [34]. Further structural inspection of the GB atoms reveals that only a small percentage are positionally disordered, that is, at positions which cannot be identified with the fcc lattice of the neighbouring grains [35]. Hence the general conclusion is, that apart from an increased triple junction density, no fundamental difference in the nc GB when compared to the polycrystalline regime exists. Indeed considerable order has been identified for particular GBs, which does not change significantly as a function of grain size [36]. Moreover some GBs (derived from the appropriate missorientation) contain clear regions of coherent and incoherent missfit, defining a GB dislocation network, that exists for a range of grain sizes [36–38].

Molecular dynamics (MD) has often been used to study the early stage of displacement cascades in metals. The sub-nanosecond time scale available to MD allows MD to address the evolution of the SIAs, but the motion of vacancies and small vacancy-clusters is outside of the MD simulation time frame.

This paper addresses the activity of SIAs during and after the cooling of the cascade in an nc Ni sample and the type of sinks that play a role in the determination of the final damage state. Two mechanisms of SIA movement, which occur during the attraction to sinks such as GBs and vacancy clusters, are temporally distinguished. The size of clusters formed relative to PKA energy introduced is discussed. The movement of large SIA clusters is presented, the sink strength of defects such as GBs and vacancy clusters is shown as well as the accommodation of the GB structure as a result of incoming SIAs.

2. Simulation and analysis technique

In the present work, computer nc samples are generated using the Voronoi [39] construction. A number of positions are randomly chosen within an empty simulation cell from which fcc lattices of differing orientation are geometrically constructed until those atoms from one grain meet atoms of another grain. Atom pairs, where each atom originates from a different grain, are inspected and if there is a nearest neighbour distance of less than 2 Å, one atom is removed. Molecular statics and MD at room temperature are then performed to

allow the structure to find the configuration closer to equilibrium [40]. For sample production MD is performed within the Parrinello–Rhaman framework [41], however during cascade simulation the volume of the system is held constant. The second moment tight binding potential of Cleri and Rosato [42] is employed. To adequately represent the hcp phase this potential extends to the fifth nearest neighbour. For cascade simulation a modification to the short range form of this potential according to Ziegler et al. [43] is used to more accurately describe the high-energy collision dynamics of the early ballistic phase. The cascade simulations were performed at room temperature, where heat was extracted via velocity rescaling of atoms within an outer cubic shell at the periodic boundary. The PKA was introduced within an nc grain situated at the centre of the simulation cell. For the present work, the simulation cell consists of 15 grains with a 12 nm mean grain diameter, constituting a total of $\sim 1 \times 10^6$ atoms in the simulation cell.

For structural analysis a medium range topological bond analysis technique [44] is adopted to aid in the visualisation of the displacement cascade and the GB structure. This allows a local crystalline symmetry to be ascribed to each atom providing a colour code scheme where fcc atoms are grey, 12-coordinated non-fcc and non 12-coordinated atoms are respectively green and blue, and first nearest neighbour hcp coordinated atoms are red spheres. Such a visualisation technique helps easy identification of twin planes via (1 1 1) hcp planes and stacking faults via two neighbouring parallel (1 1 1) hcp planes [36].

3. Results

3.1. Movement of self-intersitials to grain boundaries

The following results describe the SIA movement in a particular 5 keV cascade simulation, the chosen example being representative of other cascade simulations in the presence of GBs. The development of the cascade at particular times during the simulation is presented in Fig. 1(A)–(E), each figure showing a 'snapshot' at a particular time. Only non-fcc atoms are shown for ease of visualisation. Thus the central grain and surrounding GB structure can easily be identified, in addition to the disorder/damage resulting from the introduced PKA. In all of the figures, atomic displacement vectors, representing the duration between the initial crystalline structure (before the introduction of the PKA) and a particular time (as stated in the figure), are superimposed as pink lines onto the figures in order to further clarify atomic movement. For such displacement vectors, only those whose magnitudes are well above that expected due to thermal motion are displayed.

Fig. 1(A) presents the melt phase and movement of atoms at 0.3 ps after the introduction of the PKA. On the lower right-hand side, an RCS (labelled as RCS1) moving to a nearby GB is evident from the atomic displacement vectors with non-fcc atoms extending along its path. On the lower left-hand side, a second RCS (labelled as RCS2) appears as a similar elongated non-fcc region extending out 2.5 nm from the periphery of the cascade region. Two SIAs are thus removed from the core region by the RCS mechanism. The SIA movement induces a molten state of atoms surrounding them along the two close packed planes which they traverse, visualised here as a thin extension of the cascade core region in these directions. The cascade core, in its largest molten state, is larger than the damaged region after cooling since many displaced atoms leave their original lattice sites momentarily, becoming non-fcc during the thermal spike phase. After cooling, however, these atoms return to their original positions, transporting energy through the system as focusons. Thus the cascade core shape is affected by crystal symmetry and the velocity given to the initial PKA atom, as well as RCSs, extending the core out into a 'butterfly' shape (when viewed as a 2D projection in the appropriate orientation). The irregular shape of the disordered cascade core in the nc case is made more distinct by the presence of GB sinks which attract the RCSs.

Fig. 1(B) represents a configuration at 0.7 ps after the introduction of the PKA with the corresponding atomic displacement vectors as defined above. The two SIAs corresponding to the two RCSs identified in Fig. 1(A) have now been labelled SIA1 and SIA2. SIA1 had already arrived at the GB in Fig. 1(A) at 0.3 ps, and by 0.7 ps was observed to move further within the GB. The region to which SIA1 is attracted in the GB contains a GB dislocation where there is excess free volume obtained via theoretical positron lifetime calculations [45]. At this snapshot, not all SIAs are attracted to the various GBs by RCSs. As the cascade cools, some SIAs are left within the grain. SIA2 which has moved out towards the GB is no longer part of the cascade core, and the atoms in the region previously connecting it to the cascade core have resolidified and returned to their fcc positions, leaving SIA2 as a mono-crowdion SIA within the grain.

Fig. 1(C) represents a configuration at 5.5 ps after the introduction of the PKA with atomic displacement as described above. In this figure the core has resolidified to reveal small vacancy defects as evidenced by the surrounding blue non-12 coordinated atoms within the grain. The mono-SIA crowdion (SIA2) has changed direction and moved along one of its crowdion axes to a nearby GB within 3.1 ps of the PKA. A 6-SIA crowdion cluster containing all remaining SIAs has formed. The particular GB that attracted SIA1 and SIA2 now also biases the formation of the bigger cluster to its side of

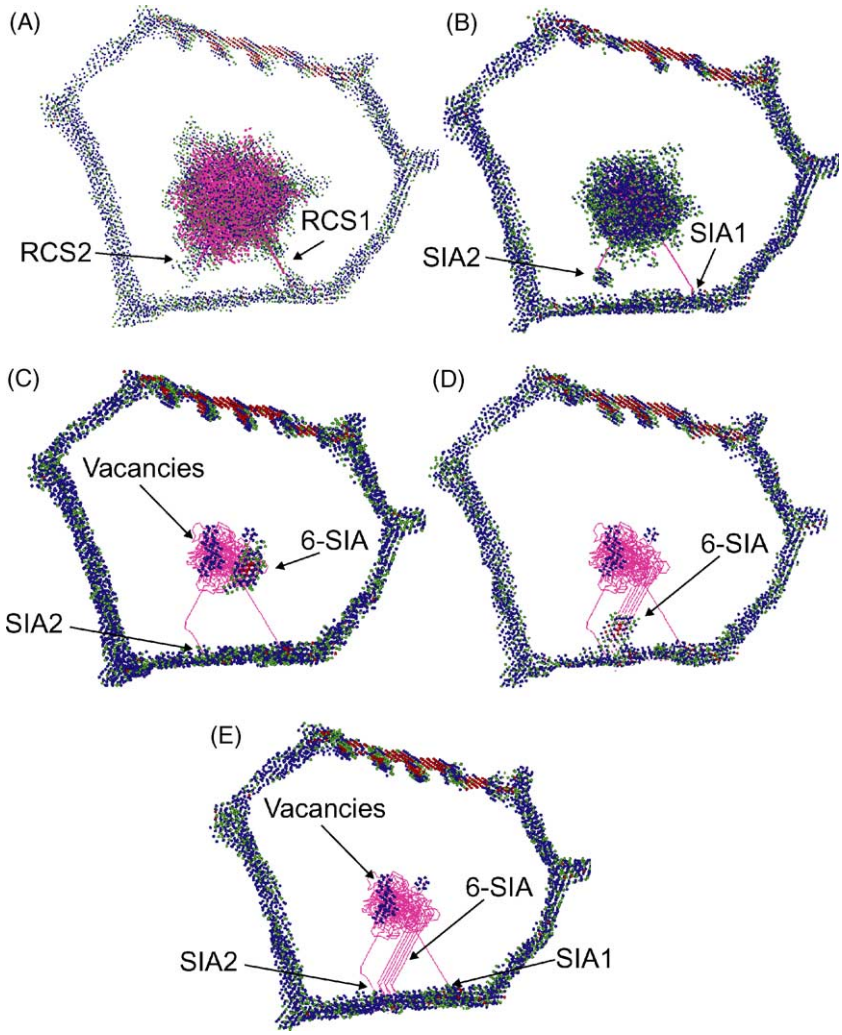

Fig. 1. Development of a 5 keV cascade in an nc grain showing the cascade (A) 0.3 ps, (B) 0.7 ps, (C) 5.5 ps, (D) 11.9 ps and (E) 13.1 ps after the introduction of the PKA. Only non-fcc atoms are shown.

the cascade core. The formation of clusters of six SIAs in single crystal 5 keV PKA cascades is rare and larger SIA clusters have not been seen [46]. The consistently large cluster sizes (up to eight SIAs in 5 keV PKA cascades) obtained in our nc simulations emphasises the interaction of GBs in cascade simulations.

Fig. 1(D) represents a configuration at 11.9 ps after the introduction of the PKA with the corresponding atomic displacement as previously stated. Here the 6-SIA crowdion cluster has moved in the direction of the GB, and by 13.1 ps has arrived at the GB via 1D/3D motion along its crowdion axis – the cluster changing its direction close to the GB between 11.9 and 13.1 ps (Fig. 1(E)) to move along another close packed plane before being absorbed by the GB. By comparison, in pure crystal samples clusters of 4 or more SIAs have been seen to move only 1D [47] re-emphasising the influence of the introduced GBs. After 13.1 ps, the remaining defects in the grain are small vacancy clusters, as all SIAs have moved to the lower GB. The implications are indicative of a GB which may have a greater 'sink strength' than the other surrounding GBs. For example, the twin GB present horizontally across the top of the grain is more coherent and therefore less likely to attract SIAs. The position of the cascade within the grain and to the surrounding GBs also plays a role in the movement of SIAs, in this case all SIAs moving to the closest GB. Another influencing factor in sink strength is the presence of a local pressure gradient within the crystalline structure which sets up a slightly positive overall pres-

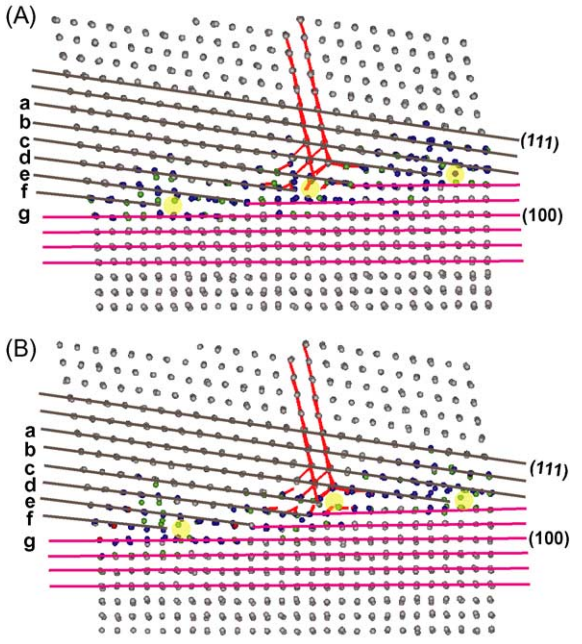

Fig. 2. Grain region at which a 6 SIA crowdion cluster is absorbed at a grain boundary dislocation. By accommodating the arriving SIAs, the grain boundary dislocation undergoes climb within the grain boundary.

sure in the grain and a slightly negative overall pressure in GB regions [48] with a consequent sink bias of GB regions.

Fig. 2(A) and (B) show a close up of the GB region at which the 6-SIA cluster seen in Fig. 1 is absorbed. The orientation of Fig. 2 is different to that of Fig. 1. Atomic displacement vectors (as described above) are also shown. In the lower grain, (1 0 0) planes are marked with magenta lines and in the upper grain, (1 1 1) planes are marked with brown lines. Lines c and e exist in both grains where the region at which a change in orientation exists is identified as a change in colour of the particular line. Lines b, d and f exist only in the upper grain, terminating at regions of misfit, or equivalently GB dislocations marked by yellow circles and correspond to regions of excess free volume [45]. This GB can therefore be described as a GB dislocation network. In both Fig. 2(A) and (B), the movement of the 6-SIA cluster is clearly evident by the red lines. Furthermore, upon entering the GB region, the SIAs look for lower density regions and therefore induce some local atomic shuffling. The absorption of six SIAs in the GB represents a local densification, and in this particular case, this is accommodated by the extension of the (1 1 1) plane d into the direction of the lower grain and a local climb of the GB dislocation (now at plane c).

At higher energy PKAs, and in cascades closer to the GB, the RCS mechanism is the primary method of removal of SIAs from the grain. A number of other displacement cascade simulations have also been performed. In a 10 keV PKA cascade situated close to a GB, all SIAs leave the grain during the thermal spike phase with no SIAs remaining within the grain on resolidification. At the end of the thermal spike phase for 20 and 30 keV PKA cascades, only a very small fraction of SIAs remain in the grain as mono- or di-SIA clusters. In this simulation the SIAs remaining in the grain after the thermal spike phase are also removed from the grain via 1D/3D motion.

3.2. Stacking fault tetrahedra as interstitial sinks

As mentioned earlier, pre-existing defects can act as sinks to mobile defects [32,49]. In this section, the sink strength of vacancy clusters, in the form of truncated SFTs (TSFT), is outlined.

We now detail a particular simulation involving the introduction of a 20 keV PKA into the nc environment in which a TSFT forms [32]. During cascade cooling, the SIAs move to the GB region during the thermal spike phase via RCSs, with the exception of two mono-SIAs. At 9.23 ps after the introduction of the PKA, the cascade core region has resolidified and two centrally located mono-SIAs, a large vacancy cluster in the shape of a TSFT, as well as a number of small free standing mono and di-vacancy clusters remain in the central grain. Between 9.23 and 17.23 ps the two mono-SIAs move towards each other and form a di-SIA cluster. Between 17.23 and 30 ps, the di-SIA cluster undergoes

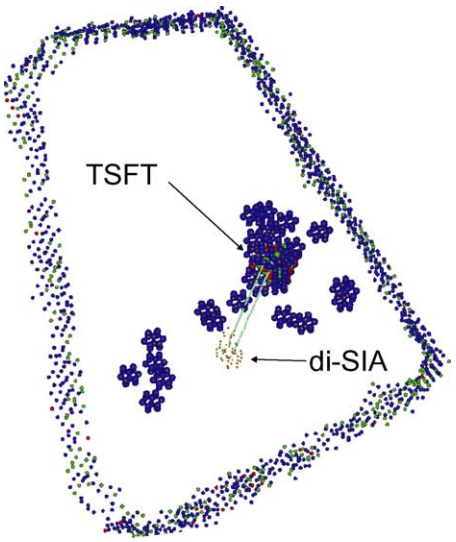

Fig. 3. Development of a 20 keV cascade in an nc grain in which a truncated stacking fault tetrahedra (TSFT) and a di-SIA cluster are created; as the cascade progresses the di-SIA moves 1D/3D and is absorbed by the TSFT.

1D/3D motion, rearranging itself along a close packed plane in which movement to the TSFT is possible via 1D motion, which it then undergoes, so that by 55.6 ps it has reached and been absorbed by the TSFT. Fig. 3 displays a section at 55.6 ps using a similar colour scheme as Fig. 1. Yellow non-fcc atoms indicate the di-SIA at 30 ps and the green atomic displacement vectors represent atomic activity between 30 and 55.6 ps. On reaching the TSFT, the SIAs move within the TSFT to regions of free volume and annihilate therein. The TSFT thus shrinks in size, acting as a sink to mobile clusters in search of the most stable configuration.

4. Conclusion

Cascade damage simulations of 12 nm grain size nc Ni reveal that sinks present in the form of grain boundaries and vacancy defects such as TSFTs play an important role in the mechanism of SIA movement. Two temporal mechanisms, replacement collision sequences and 1D/3D motion have been distinguished due to their different time dependence and as a consequence of cascade position and size relative to the surrounding GB environment. When a sink is in the vicinity of a cascade, it attracts SIAs via replacement collision sequences as part of the molten region. As the core resolidifies, the remaining SIAs form into clusters and then undergo 1D/3D motion resulting once again in their eventual absorption at a grain boundary with subsequent local restructuring of the grain boundary. The sequential evolution of a typical cascade shows that the mechanisms of RCS and 1D/3D motion are temporally distinguishable and dependent on the cascade position and size relative to the surrounding GB environment. SIA activity is biased by its interaction with the GBs present, forming clusters on the large size limit of those seen in single crystal simulations. Clusters of up to 6 SIAs are seen to undergo 1D/3D motion. In single crystal simulations such activity has been seen only in clusters of 3 SIAs or less.

Acknowledgements

M.S. acknowledges the financial support of the BBW (grant no. 98.0098) and M.V. acknowledges the financial support of the Swiss-FN (grant no. 2000-061837.00).

References

[1] B.N. Singh, A.J.E. Foreman, Philos. Mag. A 66 (1992) 975.
[2] C.H. Woo, B.N. Singh, Philos. Mag. A 65 (1992) 889.
[3] B.N. Singh, J.H. Evans, J. Nucl. Mater. 226 (1995) 277.
[4] H. Peisel, H. Trinkaus, Comm. Solid State Phys. 5 (1973) 167.
[5] R.E. Stoller, G.R. Odette, B.D. Wirth, J. Nucl. Mater. 251 (1997) 49.
[6] P. Zhao, Y. Shimimura, Comp. Mater. Sci. 14 (1999) 84.
[7] H. Trinkaus, B.N. Singh, A.J.E. Foreman, J. Nucl. Mater. 199 (1992) 1.
[8] H. Trinkaus, B.N. Singh, A.J.E. Foreman, J. Nucl. Mater. 206 (1993) 200.
[9] A.J.E. Foreman, C.A. English, W.J. Phythian, Philos. Mag. A 66 (1992) 655.
[10] Yu.N. Osetsky, A. Serra, V. Priego, J. Nucl. Mater. 276 (2000) 202.
[11] H.L. Heinisch, B.N. Singh, S.I. Golubov, J. Nucl. Mater. 276 (2000) 59.
[12] Yu.N. Osetsky, M. Victoria, A. Serra, S.I. Golubov, V. Priego, J. Nucl. Mater. 251 (1997) 34.
[13] T. Diaz de la Rubia, M. Guinan, Phys. Rev. Lett. 66 (1991) 2766.
[14] D.J. Bacon, T. Diaz de la Rubia, J. Nucl. Mater. 216 (1994) 275.
[15] N. Soneda, T. Diaz de la Rubia, Philos. Mag. A 78 (1998) 995.
[16] F. Gao, D.J. Bacon, Yu.N. Osetsky, P.E.J. Flewitt, T.A. Lewis, J. Nucl. Mater. 276 (2000) 213.
[17] B.D. Wirth, V. Bulatov, T. Diaz de la Rubia, J. Nucl. Mater. 283–287 (2000) 773.
[18] S.L. Dudarev, Phys. Rev. B 65 (2002) 224105.
[19] B.N. Singh, S.J. Zinkle, J. Nucl. Mater. 206 (1993) 212.
[20] H. Trinkaus, B.N. Singh, A.J.E. Foreman, J. Nucl. Mater. 251 (1997) 172.
[21] B.N. Singh, A.J.E. Foreman, H. Trinkaus, J. Nucl. Mater. 249 (1997) 103.
[22] N.M. Ghoniem, B.N. Singh, L.Z. Sun, T. Diaz de la Rubia, J. Nucl. Mater. 276 (2000) 166.
[23] W. Sigle, M.L. Jenkins, L.J. Hutchison, Philos. Mag. Lett. 57 (1988) 267.
[24] H. Trinkaus, B.N. Singh, A.J.E. Foreman, J. Nucl. Mater. 249 (1997) 91.
[25] E. Kuramoto, K. Ohsawa, T. Tsutsumi, J. Nucl. Mater. 283–287 (2000) 778.
[26] M. Samaras, P.M. Derlet, H. Van Swygenhoven, M. Victoria, Phys. Rev. Lett. 88 (2002) 125505.
[27] K. Sugio, Y. Shimomura, T. Rubia, J. Phys. Soc. Jpn. 67 (1998) 882.
[28] M. Samaras, P.M. Derlet, H. Van Swygenhoven, M. Victoria, Philos. Mag. A, in press.
[29] A.P. Sutton, R.W. Ballufi, Interfaces in Crystalline Materials, Clarendon, Oxford, 1995.
[30] Y. Chimi, A. Iwase, N. Ishikawa, M. Kobiyama, T. Inami, S. Okuda, J. Nucl. Mater. 297 (2001) 355.
[31] M. Rose, A.G. Balogh, H. Hahn, Nucl. Instrum. and Meth. B 127&128 (1997) 119.
[32] M. Samaras, P.M. Derlet, H. Van Swygenhoven, M. Victoria, Nucl. Instrum. and Meth. B 202 (2003) 51.
[33] A. Caro, H. Van Swygenhoven, Phys. Rev. B 63 (2001) 134101.
[34] H. Van Swygenhoven, A. Caro, Phys. Rev. B 58 (1999) 17.
[35] P.M. Derlet, H. Van Swygenhoven, Phys. Rev. B 67 (2003) 014202.

[36] H. Van Swygenhoven, D. Farkas, A. Caro, Phys. Rev. B 62 (2000) 831.
[37] H. Van Swygenhoven, Science 296 (2002) 66.
[38] H. Van Swygenhoven, P.M. Derlet, Phys. Rev. B 64 (2001) 224105.
[39] G.Z. Voronoi, J. Reine. Angew. Math. 1 (34) (1908) 199.
[40] H. Van Swygenhoven, M. Spaczer, A. Caro, Acta Mater. 47 (1999) 3117.
[41] M. Parrinello, A. Rahman, J. Appl. Phys. 52 (1981) 7182.
[42] F. Cleri, V. Rosato, Phys. Rev. B 48 (1993) 22.
[43] J. Ziegler, J.P. Biersack, U. Littmark, The Stopping Range of Ions in Solids, Pergamon, New York, 1987.
[44] D.J. Honeycutt, H.C. Andersen, J. Phys. Chem. 91 (1987) 4950.
[45] S. Van Petegem, Positron annihilation study of nanocrystalline materials, doctoral thesis, University of Ghent, 2003.
[46] D.J. Bacon, A.F. Calder, F. Gao, J. Nucl. Mater. 251 (1997) 1.
[47] D.J. Bacon, F. Gao, Yu.N. Osetsky, J. Nucl. Mater. 716 (2000) 1.
[48] A. Hasnaoui, H. Van Swygenhoven, P.M. Derlet, Acta Mater. 50 (2002) 3927.
[49] C.A. English, W.J. Phythian, A.J.E. Foreman, J. Nucl. Mater. 174 (1990) 135.